DOI: 10.1002/ejic.200801153

Structural Flexibility and Selective Guest Accommodation in Two Cu^{II} Metal–Organic Coordination Frameworks

Kargal L. Gurunatha[a] and Tapas Kumar Maji*[a]

Keywords: Host–guest systems / Flexible frameworks / Adsorption / Copper / Magnetic properties

Two metal–organic coordination frameworks of Cu^{II}, $[Na_2Cu(2,4\text{-pyrdc})(H_2O)(\mu\text{-}OH_2)_2]_n$ (**1**) and $\{[Cu(2,5\text{-pyrdc})(NH_3)](2H_2O)\}_n$ (**2**) (2,4-pyrdc = pyridine-2,4-dicarboxylate; 2,5-pyrdc = pyridine-2,5-dicarboxylate), were synthesized and structurally characterized. The structure of compound **1** was known and shows that $Cu(2,4\text{-pyrdc})_2(H_2O)$ functions as a metalloligand and is linked to two different Na^I atoms to form a 3D heterometallic Cu^{II}–Na^I framework. The single crystals of compound **2** were obtained from aqueous ammoniacal solution and crystallize in the triclinic ($P\bar{1}$) crystal system. Compound **2** is a 2D sheet consisting of two different Cu^{II} 1D chains bridged by a 2,5-pyrdc ligand. Stacking of the 2D sheets results in a 3D supramolecular host with 1D water-filled channels. Both frameworks are highly thermally stable and exhibit reversible structural transformation upon removal of the metal-bound water and NH_3 molecules for **1** and **2**, respectively. Sorption studies reveal that desolvated frameworks **1′** and **2′** both behave nonporous to N_2. However, **1′** exhibits structural transformation and hysteretic stepwise sorption of H_2O and MeOH molecules, but THF and C_6H_6 molecules are not adsorbed. Similarly, H_2O and MeOH molecules are easily adsorbed in **2′**, but THF and C_6H_6 molecules are not. Such high selectivity in **1′** and **2′** was correlated to the smaller pore aperture and specific host–guest interaction conferred by the unsaturated Lewis acidic sites on the pore surfaces and the Lewis basic adsorbates. Low-temperature magnetic study of **2** revealed that the Cu^{II} atoms are antiferromagnetically coupled, with J = –1.45 cm^{-1} and g = 2.01.

Introduction

The last decade has seen enormous research efforts in the synthesis and studies of metal–organic coordination frameworks and continuing to expand exponentially due to their novel structural topology and interesting physical and chemical properties.[1] In particular, frameworks with permanent porosity have attracted the attention of chemists, physicists, as well as materials scientists due to their scientific interest in the creation of nanometer-sized spaces for investigating novel phenomena,[2] as well as commercial interest in their application for gas storage (like H_2, CH_4)[3] and in heterogeneous catalysis.[4] Rigid and robust porous frameworks with a high surface area and different degrees of sorption and separation characteristics are now well established.[2,3] However, flexible frameworks, classified as a third generation of porous frameworks by Kitagawa et. al,[5] exhibit dynamic behavior, such as single-crystal-to-single-crystal,[6] crystal-to-amorphous,[7] guest responsive structural transformation,[8] and selective sorption of specific molecules.[9] Therefore, the creation of a host framework that can interact with the selective guest molecules has significance for molecular separations and sensing. To satisfy the desired coordination geometry, the host framework can also coordinate to the solvent molecules of the reaction medium. Upon removal of the metal-bound solvent molecules, the resulting desolvated framework with unsaturated coordination sites can interact with the specific guest molecules.[10] However, the facilitation of the diffusion of a specific guest species in the vapor state by a crystalline nonporous solid is not a common phenomenon. This kind of structural motion, where the nonporous phase opens up the channel aperture for accommodation of the guest molecules, is driven by external stimuli such as temperature, pressure, and light.[6e,11] In addition, the sorption in a nonporous molecular crystal is also impelled by the strong host–guest interaction; for example, Lewis acid–base interaction with ultimate formation of metal–ligand covalent bonds can compensate the energy for structural rearrangement.[12] Recent developments have exhibited that selective guest accommodation is feasible by specific interactions such as H-bonding or coordination covalent bonds.[13] In this manuscript we report the synthesis and structural characterization and guest-induced structural rearrangement of two metal–organic coordination frameworks, $[Na_2Cu(2,4\text{-pyrdc})(H_2O)(\mu\text{-}OH_2)_2]_n$ (**1**) and $\{[Cu(2,5\text{-pyrdc})(NH_3)](2H_2O)\}_n$ (**2**) (2,4-pyrdc = pyridine-2,4-dicarboxylate and

[a] Molecular Materials Laboratory, Chemistry and Physics of Materials Unit Jawaharlal Nehru Centre for Advanced Scientific Research,
Jakkur, Bangalore 560064, India
Fax: +91-80-2208-2766
E-mail: tmaji@jncasr.ac.in

Supporting information for this article is available on the WWW under http://www.eurjic.org or from the author.

2,5-pyrdc = pyridine-2,5-dicarboxylate). The structure of the 3D nonporous heterometallic (Cu^{II} and Na^{I}) framework of **1** was first reported by Sileo et al.[14] We consequently prepared this compound and investigated the dynamic and flexible behavior of this material; it exhibits a highly selective guest-induced structural transformation and gated-sorption behavior. Framework **2** is a 2D coordination network consisting of two different Cu^{II} centers; the 2D sheets are connected through H-bonds to form a 3D supramolecular framework with 1D water-filled channels. Framework **2** demonstrates size-selective sorption properties and displays weak antiferromagnetic interactions at low temperature realized by the *syn–anti* carboxylate bridges between the Cu^{II} centers.

Results and Discussion

IR Spectroscopy

The IR spectrum of **1** shows sharp bands at 3440 and 3350 cm^{-1}, corresponding to ν(O–H) of the coordinated water molecules, and **2** shows a broad band around 3440 cm^{-1} and a sharp band at 3245 cm^{-1}, which can be assigned to the ν(O–H) of the water molecule and ν(N–H) of the coordinated NH_3 molecules, respectively (Figure S1, Supporting Information).[15] The noncoordinated dicarboxylate ligand shows a strong ν_{as}(OCO) band at 1700 cm^{-1} and a ν_{s}(OCO) band at 1450 cm^{-1}.[15] It also shows two medium-intensity bands at 800 and 750 cm^{-1} assigned to the OCO bending frequencies. The frequencies associated with the 2,4-pyrdc and 2,5-pyrdc ligands are significantly shifted to lower frequencies upon coordination to the Cu^{II} ions. In **1** the [ν_{as}(OCO)] and [ν_{s}(OCO)] bands appear at 1554 and 1394 cm^{-1} and for **2** at 1563 and 1388 cm^{-1}, respectively. The absence of bands at around 1700 cm^{-1} in **1** and **2** indicates that carboxylate groups are involve in coordination with the Cu^{II} ions (Figure S1, Supporting Information).

Structural Description of $[Na_2Cu(2,4\text{-pyrdc})(H_2O)(\mu\text{-}OH_2)_2]_n$ (1)

Compound **1** is a 3D heterometallic Na^{I} and Cu^{II} framework bridged by 2,4-pyrdc and H_2O, with the formulation $[Na_2Cu(2,4\text{-pyrdc})(H_2O)(\mu\text{-}OH_2)_2]_n$. The structure of compound **1** was reported by Sileo et al.,[14] and some of the salient features of the framework follow: Each square pyramidal Cu^{II} ion is chelated to two different 2,4-pyrdc ligands and ligated to one water molecule in the axial position to form a Cu(2,4-pyrdc)$_2$(H_2O) metalloligand (Figure 1a).[16] Each Cu(2,4-pyrdc)$_2$(H_2O) metalloligand is connected to six different Na^{I} atoms through the pendent carboxylate oxygen atoms to form a 3D coordination framework (Figure 1b). One 2,4-pyrdc ligand is chelated to Na1 (O8, O9), and it is also attached to two different Na2 atoms through the carboxylate oxido bridges (μ_2-O8 and μ_2-O9). Another 2,4-pyrdc ligand of the metalloligand is chelated to Na2 (O4, O5) and also attached to two different Na1 atoms through the μ_3-O5 carboxylate oxygen atom (Figure 1a). Therefore, both 2,4-pyrdc ligands act as tetradentate ligands. The Na1 and Na2 atoms are both hexacoordinate and bridged by the two water molecules (O10, O11) to form a purely inorganic Na–O–Na 2D corrugated sheet in the crystallographic *bc* plane (Figure 2a). The Cu(2,4-pyrdc)$_2$ units are aligned in a parallel manner along the crystallographic *b* and *c* axes and are separated by the Na–O–Na layer (Figure 1b). The overall structure is reinforced by π–π interactions (cg···cg distances 3.606–4.156 Å) and several H-bonding interactions between the coordinated water molecules and the carboxylate oxygen atoms [2.692(2)···

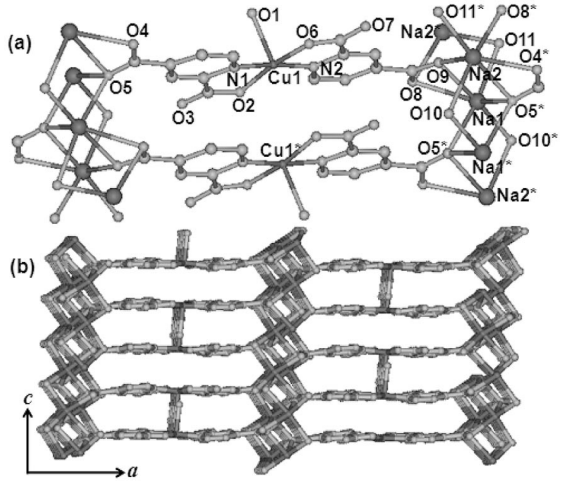

Figure 1. (a) View of the coordination environment around Cu^{II} and Na^{I} in framework **1**; (b) view of the 3D coordination framework of **1** along the crystallographic *b* axis.

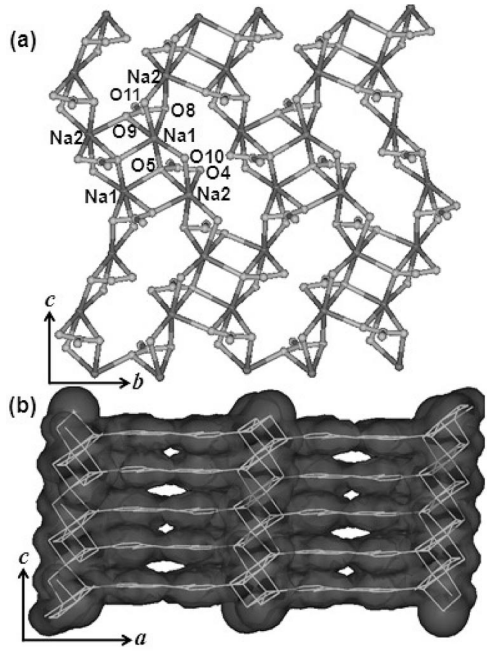

Figure 2. (a) View of the 2D inorganic layer with Na–O–Na connectivity in the crystallographic *bc* plane; (b) view of the 3D network of **1** showing a very narrow channel along the *b* axis with coordinatively unsaturated Cu^{II} sites.

2.931(2) Å] (Table S2, Supporting Information). The nearest-neighbor Cu···Cu separation along the *c* axis is 3.767 Å and along the *b* axis it is 8.322 Å. The Na···Na separations along the water bridge are (O10) 3.608 Å and (O11) 3.464 Å, and along the oxido bridge (μ-O5) 3.628 Å. Upon removal of the coordinated water molecules, the metal [Cu^{II} and Na^{I}] sites become coordinatively unsaturated, resulting in the formation of a small channel (1.0×0.4 Å^2)[17] along the crystallographic *b* axis (Figure 2b). Selected bond lengths and angles of **1** are given in Table S1 (Supporting Information).

Structural Description of {[Cu(2,5-pyrdc)(NH$_3$)]-(2H$_2$O)}$_n$ (2)

Compound **2** crystallizes in the triclinic $P\bar{1}$ space group, and its structure determination reveals that the asymmetric unit comprises two Cu^{II} ions located in special positions, one bridging 2,5-pyrdc ligand, one NH_3 molecule, and two crystalline guest water molecules (Figure 3). Each Cu1 atom is connected to two different 2,5-pyrdc ligands through the monodentate carboxylate oxygen atoms [O1, O1_c; *c* = 1 –*x*, –1 – *y*, 3 – *z*; Cu1–O1 2.007(3) Å] and two nitrogen atoms [N1, N1_b; *b* = 1 + *x*, *y*, *z*; Cu1–N1 1.975(3) Å] from the NH_3 ligands in the equatorial positions, and the axial positions are occupied by two monodentate carboxylate oxygen atoms [O2_a, O2_d; a = –1 + *x*, *y*, *z*; d = 2 –*x*, –1 – *y*, 3 – *z*; Cu1–O2 2.599(3) Å] from another two different 2,5-pyrdc ligands. Whereas 4+2 coordination around the Cu2 atom is completed by the two chelated 2,5-pyrdc ligands in the equatorial positions [N2, O3, and N2_e, O3_e; e = 2 – *x*, –*y*, 2 – *z*; Cu2–N2 1.977(3) and Cu2–O3 1.932(3) Å] and two monodentate carboxylate oxygen atoms (O4_a, O4_f; a = –1 + *x*, *y*, *z*; f = 3 – *x*, –*y*, 2 – *z*) from another two 2,5-pyrdc ligands in the axial positions. The degree of distortion from the ideal octahedral geometry is reflected in the *cisoid* angles 86.64(13)–93.37(13)° and 84.33(8)–95.67(8)° for Cu1 and Cu2, respectively. Each Cu1 atom is attached to another two nearest neighbor Cu1 centers through *syn–anti* carboxylate bridges to form 1D Cu1 chains, and Cu2 is also ligated with two nearest Cu2 centers in a *syn–anti* fashion to form 1D Cu2 chains. The 1D Cu1 and Cu2 chains are bridged by the 2,5-pyrdc ligand to form 2D corrugated sheets lying in the crystallographic *ac* plane (Figure 3). The distances between Cu1···Cu1 and Cu2···Cu2 are the same 4.966 Å, and the nearest Cu1···Cu2 distance is 7.440 Å (Table 1). 2D sheets stack along the crystallographic *a* axis to produce dumbbell-shaped channels occupied by the two water molecules (Figure 4). The water molecules are H-bonded to each other [O5···O6 2.699(6)–2.833(6) Å] and also to the coordinated NH_3 molecules [N–H1···O6 2.968(5) Å] (Table 2) to form a 3D supramolecular framework (Figure 4a).

Table 1. Selected bond lengths [Å] and bond angles [°] for **2**.[a]

Cu1–O1	2.007(3)	Cu2–O3	1.932(3)
Cu1–N1	1.975(3)	Cu2–N2	1.977(3)
Cu1–O2_a	2.599(3)	Cu2–O4_a	2.753(4)
Cu1–O1_c	2.007(3)	Cu2–O3_e	1.932(3)
Cu1-01_c	1.975(3)	Cu2–N2_e	1.977(3)
Cu1–O2_d	2.599(3)	Cu2–O4_f	2.753(4)
O1–Cu1–N1	93.37(13)	O3–Cu2–N2	84.33(8)
O1–Cu1–O2_a	92.46(7)	O3–Cu2–O4_a	91.56(7)
O1–Cu1–O1_c	180	O3–Cu2–O*3_e	180
O1–Cu1–N1_c	86.64(13)	O3–Cu2–N2_e	95.67(8)
O1–Cu1–O2_d	87.54(7)	O3–Cu2–O4_f	88.44(7)
O2_a–Cu1–N1	89.47(11)	O4_a–Cu2–N2	87.74(8)
O1_c–Cu1–N1	86.64(13)	O3_e–Cu2–N2	95.67(8)
N1–Cu1–N1_c	180	N2–Cu2–N2_e	180
O2_d–Cu1–N1	90.53(11)	O4_f–Cu2–N2	92.26(8)
O1_c–Cu1–O2_a	87.54(7)	O3_e–Cu2–O4_a	88.44(7)
O2_a–Cu1–N1_c	90.53(11)	O4_a–Cu2–N2_e	92.26(8)
O2_a–Cu1–O2_d	180	O4_a–Cu2–O4_f	180
O1_c–Cu1–N1_c	93.37(13)	O3_e–Cu2–N2_e	84.33(8)
O1_c–Cu1–O2_d	92.46(7)	O3_e–Cu2–O4_f	91.56(7)
O2_d–Cu1–N1_c	89.47(11)	O4_f–Cu2–N2_e	87.74(8)

[a] Symmetry code: a: –1 + *x*, *y*, *z*; *c*: 1 – *x*, –1 – *y*, 3 – *z*; d: 2 – *x*, –1 – *y*, 3 – *z*; e: 2 – *x*, –*y*, 2 – *z*; f: 3 – *x*, –*y*, 2 – *z*.

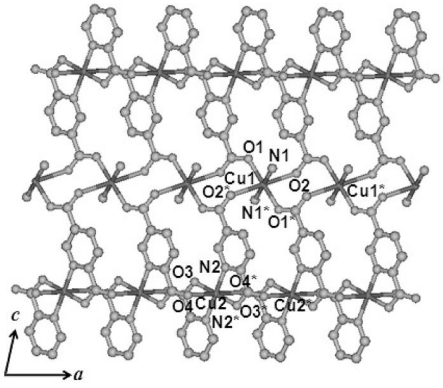

Figure 3. View of the coordination environment of Cu1 and Cu2 in the 2D sheet lying in the crystallographic *ac* plane.

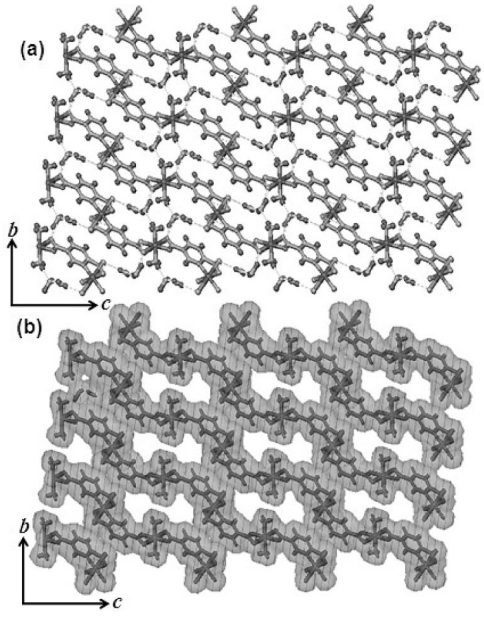

Figure 4. View of the 3D supramolecular framework of **2** (a) along the *a* axis showing channel water molecules are connecting the 2D sheet through H-bonding; (b) dumbbell-shaped 1D channels along the crystallographic *a* axis generated upon the stacking of the 2D sheet.

Table 2. Hydrogen bonds for **2**.[a]

D–H···A	D–H [Å]	H···A [Å]	D···A [Å]	<D–H···A [°]
N1···H1···O6^{i}	0.88(6)	2.11(6)	2.968(5)	163(5)
O5···H7···O6^{ii}	0.81(5)	2.06(5)	2.833(6)	162(4)
O5···H8···O4	0.68(4)	2.14(4)	2.807(5)	174(6)
O6···H9···O5^{iii}	1.00(7)	1.76(6)	2.699(6)	155(5)
O6···H10···O2	1.23(7)	1.62(8)	2.794(5)	158(6)
C4···H5···O4^{iii}	0.76(4)	2.53(4)	3.226(5)	154(4)

[a] Symmetry code: i: 2 – *x*, –2 – *y*, 3 – *z*; ii: 3 – *x*, –1 – *y*, 2 – *z*; iii: 4 – *x*, –1 – *y*, 2 – *z*.

The size of the dumbbell-shaped channel is about 3.4×3.8 Å^2 (Figure 4b),[17] which would be modified to rectangular channels of about 3.8×8.2 Å^2 after removal of the coordinated NH_3 molecules (Figure S2, Supporting Information).

Framework Stability: TGA and PXRD Analyses

As seen from structural analysis, compound **1** includes three coordinated water molecules; one is attached to the Cu^{II} atom and other two are involved in bridging the Na^{I} atoms. TGA shows that all three water molecules are released in between 120 and 155 °C, and the dehydrated framework (i.e., **1′**) is stable up to 280 °C (Figure S3, Supporting Information). The weight loss (obs. 10.86 wt.-%) is consistent with the three water molecules (calcd. 10.93 wt.-%). In the case of **2**, guest water and metal-bound NH_3 molecules are removed in a stepwise fashion (Figure S3, Supporting Information). The first step from room temperature to 75 °C corresponds to the loss of one water molecule (obs. 5.91 wt.-%; calcd. 6 wt.-%) and the second step at 75–115 °C is associated with the release of NH_3 molecules. Desolvated framework **2′** is stable up to 270 °C without any weight loss. The powder X-ray diffraction (PXRD) pattern of **1′** shows sharp lines with shifting of the peak position (peaks at 2θ = 11.36 moves to 11.66) and also the disappearance of some peaks (2θ = 12.72) in comparison to the as-synthesized framework **1**, suggesting structural transformation after removal of the metal-bound water molecules (Figure 5), rather than collapse of the framework. Indexing of the powder pattern of **1′** by using the TREOR program[18] suggests a = 15.66(2) Å; b = 12.757(9) Å; c = 7.634(8) Å; β = 93.63(15)°, and V = 1522.66 Å^3, which is indicative of structural contraction upon dehydration (Table S2, Supporting Information).

When **1′** was exposed to water vapor for 3 d the virgin framework regenerated, suggesting the reversibility of water coordination (Figure 5). The PXRD pattern of **2′** exhibits the appearance of some new peaks at around 2θ = 2.3, 9.0, 15.2 and the other peaks remain in the same positions, which lead to a framework with unsaturated Cu^{II} sites (Figure 6). Indexing of the powder pattern of **2′** leads to a = 13.914(5) Å, b = 11.442(7) Å, c = 9.846(6) Å, β = 106.21(3)°, and V = 1505.25 Å^3, corroborating substantial structural changes after removal of the guest water and coordinated NH_3 molecules. When desolvated framework **2′** was exposed to the aqueous NH_3 vapor, as-synthesized framework **2** was regenerated (Figure 6).

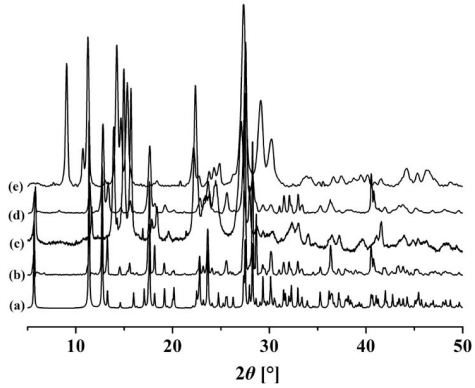

Figure 5. PXRD pattern of **1** in different states: (a) simulated; (b) as-synthesized; (c) dehydrated at 160 °C; (d) rehydrated; (e) exposed to MeOH for 3 d.

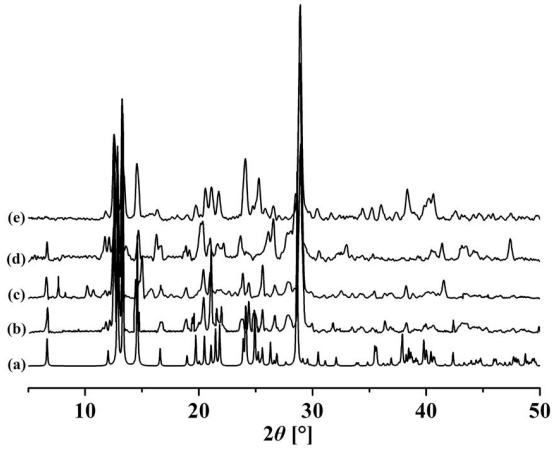

Figure 6. PXRD pattern of **2** in different states: (a) simulated; (b) as-synthesized; (c) dehydrated at 120 °C; (d) exposed to aqueous NH_3; (e) exposed to MeOH for 3 d.

Adsorption Properties

Structural analysis of **1** suggests the framework has no open channel and N_2 (kinetic diameter = 3.6 Å)[19,20] sorption isotherm for **1′** at 77 K reveals no uptake into the framework but only surface adsorption (Figure S4, Supporting Information). However, the N_2 sorption profile for **2′** shows a type II profile and the sorption amount increases with increasing pressure, suggesting adsorption on the surface rather than in the pores, which may be distorted after removal of the guest water and coordinated NH_3 molecules. Therefore, frameworks **1′** and **2′** are both nonporous with respect to N_2 sorption studies. The excellent framework stability with coordinatively unsaturated metal sites of both compounds (for **1′** and **2′**) provides an opportunity to perform solvent vapor sorption studies with solvents of different polarities to establish the sorption affinity and selectivity in both frameworks. When **1′** was exposed to MeOH

vapor for 3 d, a drastic color change from sky blue to violet was observed (Figure S5, Supporting Information). The sorption study of MeOH (kinetic diameter = 4.0 Å)[19–20] at 298 K is shown in Figure 7, which exhibits no uptake of MeOH up to P/P_0 = 0.4, but adsorption then gradually started to occur, and at P/P_0 = 0.6, the amount is 16 mL g^{-1}. Afterwards, a steep uptake of MeOH molecules up to P/P_0 = 0.74 was observed and finally ended with 142 mL g^{-1} at P/P_0 = 0.96 without saturation. The desorption curve does not follow the adsorption curve and shows large hysteresis; all the MeOH molecules cannot be desorbed from the framework (desorption curve up to P/P_0 = 0.1), which suggests that the MeOH molecules bind strongly to **1′**. The sudden adsorption jump in MeOH sorption at a certain pressure, called the gate-opening pressure,[11,12a] correlates to the structural transformation, which is driven by the three coordinated unsaturated Lewis acidic sites lying on the surface of **1′**. The PXRD pattern of the sample of **1′** exposed to MeOH (Figure 5e) reveals a drastic change with generation of new peaks (2θ = 9.8, 11.23, etc.) and disappearance of some peaks (such as low-angle peak, 2θ = 5.8), suggesting significant structural modification upon MeOH inclusion. The Dubinin–Radushkevich (DR) equation[21] suggests that 2.75 molecules of MeOH were accommodated per formula unit, with nearly one MeOH molecule per unsaturated site. MeOH sorption study in framework **2′** reveals gradual uptake with increasing pressure with a small kink at P/P_0 = 0.23 and finally shows 72 mL g^{-1} without saturation (Figure 8). The desorption curve does not trace the adsorption curve and shows large hysteresis and incomplete desorption in the low-pressure region, suggesting strong confinement of the MeOH molecules in the pore surfaces with the coordinatively unsaturated Lewis acidic Cu^{II} sites. The DR equation suggests that 1.2 molecules of MeOH were included per unit of **2′**. The PXRD pattern of the MeOH-dosed sample exhibits the appearance and disappearance of some peaks as well as changes in the Bragg intensity, which correlates the structural transformation with the accommodation of large MeOH molecules (Figure 6e). The values of βE_0, which reflect the adsorbate–adsorbent affinity, for MeOH sorption are 2.70 and 2.48 kJ mol^{-1} for **1′** for **2′**, respectively. Dehydrated frameworks **1′** and **2′** both exhibit stepwise hysteretic H_2O sorption (Figure S6, Supporting Information) and steep uptake in the low-pressure region in comparison to MeOH sorption, which in both cases suggests strong affinity to the H_2O molecules in the pore surfaces decorated with coordinatively unsaturated Cu^{II} sites. The βE_0 values for H_2O sorption are 6.66 and 7.58 kJ mol^{-1} for **1′** and **2′**, respectively, suggesting **2′** is more hydrophilic in nature.

Guest selectivity in **1′** and **2′** was examined for organic vapors with or without Lewis basicity like THF (kinetic diameter = 5.4 Å)[19,20] and C_6H_6 (kinetic diameter = 5.8 Å), respectively. Frameworks **1′** and **2′** were exposed to the organic vapor THF and C_6H_6 for 3 d, exhibiting no color change, and the PXRD patterns are shown in Figures S7 and S8, respectively, for **1′** and **2′**. In both cases, the THF and C_6H_6 exposed sample showed no change in

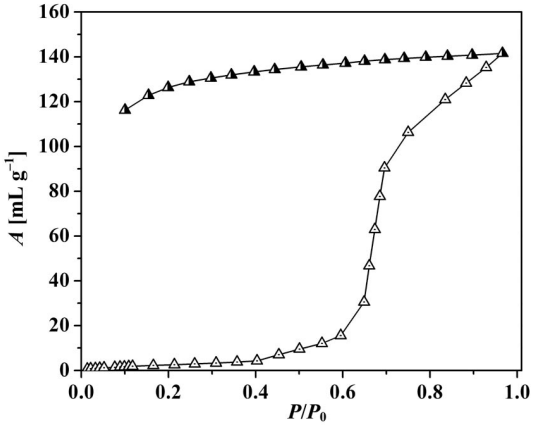

Figure 7. MeOH sorption profile for **1′** at 298 K. P_0 is the saturated vapor pressure of MeOH at the respective temperature.

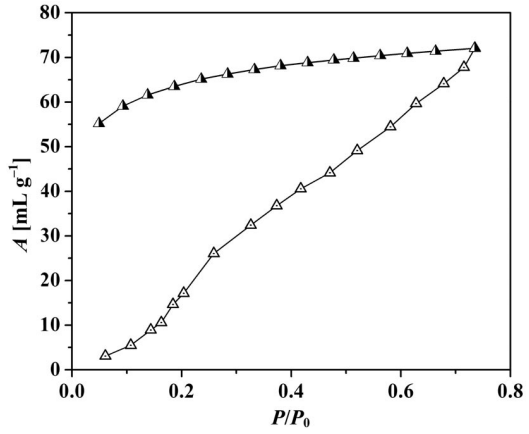

Figure 8. MeOH sorption profile for **2′** at 298 K. P_0 is the saturated vapor pressure of MeOH at the respective temperature.

the peak positions and the relative intensities were identical to those of desolvated frameworks **1′** and **2′**, indicating noninclusion of the THF and C_6H_6 molecules. This type of highly selective adsorption can be correlated with the size and shape and weak Lewis basicity of THF or C_6H_6 in comparison to the MeOH molecules. Frameworks **1** and **2** both provide Lewis acidic sites after removal of the coordinated water and NH_3 molecules, respectively. This observation correlates the very high selectivity towards the MeOH molecules. Here, the selective sorption of an organic vapor guest by a nonporous molecular crystal is driven by the size, the coordinating and the H-bonding ability of the guest molecules. H_2O and MeOH are smaller in size in comparison to THF or C_6H_6 and have profound H-bonding capability with the carboxylate oxygen atoms of the host solid, resulting in higher affinity towards the pore surfaces. This type of sorption requires substantial structural rearrangement within the crystalline solid including the change in the Cu^{II} coordination environment. However, there is a remarkable difference between **1′** and **2′** in the process of adsorption and desorption of MeOH. In the case of **1′**, gated sorption can be correlated with a highly reactive surface with

coordinatively unsaturated Cu^{II} and Na^{I} sites, which provide accommodation without having effective channels. In the case of **2′**, after removal of the of H_2O and NH_3 molecules the above-mentioned 1D channels form, and as a result of this regularity the uptake of MeOH into the framework can gradually start to occur.

Magnetic Properties of 2

The temperature dependence (300–2.4 K) of χ_M and $\chi_M T$ plots (χ_M being the magnetic susceptibility for one Cu^{II} ion) for **2** are shown in Figure 9. The χ_M value of **2** at 300 K is 0.00146 $cm^3 mol^{-1}$ ($\chi_M T$ = 0.437 $cm^3 mol^{-1} K$) and the values which is as expected for a magnetically "isolated" Cu^{II} ion. With a decrease in the temperature, the values of χ_M increase and from room temperature to 30 K (0.00987 $cm^3 mol^{-1}$ for **2** at 30 K) there is a smooth increase, and from 30 to 2.4 K the increase is more pronounced (χ_M = 0.10164 $cm^3 mol^{-1}$ at 2.4 K). The $\chi_M T$ product gradually decreases when cooling, and at 11 K, the value is 0.283 $cm^3 mol^{-1} K$ and then steeply decreasing to 0.247 $cm^3 mol^{-1} K$ at 2.4 K. There are no maxima in the χ_M versus T curve and the shape of the $\chi_M T$ versus T curve is characteristic for the occurrence of weak antiferromagnetic interactions between the Cu^{II} centers. It has already been reported that the magnetic interaction through the 2,5-pyrdc ligand connected by the two different carboxylate ligands is negligible due to the long distances between the magnetic centers (distance between Cu1 and Cu2 for **2** is 7.44 Å).[22] Therefore, the important magnetic pathways in **2** are the 1D Cu^{II} chains [(Cu1–(O1–C1–O2)$_2$–Cu1)$_n$] and [(Cu2–(O3–C6–O4)$_2$–Cu2)$_n$] bridged by the carboxylate groups of the 2,5-pyrdc ligand in *syn–anti* binding modes (Cu1···Cu1 and Cu2···Cu2 distances are the same 4.97 Å). Thus, their magnetic behaviors can be simulated by the Bonner–Fisher uniform antiferromagnetic Heisenberg chain model by using the effective spin Hamiltonian $H = JS_iS_{i+1}$.[23] The least-square fit leads to the following parameters: J = –1.85 cm^{-1}, g = 2.02, $TIP = 120.0 \times 10^{-6}$, and $R = 2.43 \times 10^{-6}$ [where $R = \Sigma(\chi_M T_{obs.} - \chi_M T_{calcd.})^2 / \Sigma(\chi_M T_{calcd.})^2$], which actually corresponds to an excellent experiment–theory agreement.

The carboxylate group can adopt three different *syn–syn*, *syn–anti*, and *anti–anti* bridging conformations. Antiferromagnetic coupling is observed in the case of *syn–syn* and *anti–anti* bridging conformations, whereas weak ferro- or antiferromagnetic interactions are found with the *syn–anti* binding modes.[24] The sign of the interactions, that is, ferro- or antiferromagnetic interactions, depends on the overlap between the interacting magnetic orbitals of the metal ions and those of the atoms of the bridge.[24c] The strong overlap in *syn–anti* binding mode of the carboxylate bridges provide antiferromagnetic interactions, and poor overlap results in a very small antiferromagnetic contribution, which results in the ferromagnetic contribution to be dominant.[24b] Both the Cu1 and Cu2 atoms are in a 4+2 coordination environment, and the magnetic orbitals are of the $d_{x^2-y^2}$ type. In the *syn–anti* carboxylate bridge, one of the oxygen atoms is in the equatorial position to one Cu1/Cu2 and the other oxygen atoms are in axial positions to the next Cu1/Cu2 atoms. Therefore, if the carboxylate bridges were of equatorial and axial type, the magnetic coupling would be between $d_{x^2-y^2}$ and d_{z^2}, and the latter orbital has very low electron density. The overlap integral between two of these orbitals through the *syn–anti* carboxylate bridge is expected to be very small; consequently, the antiferromagnetic coupling is also predicted to be smaller, which is experimentally observed in compound **2**.

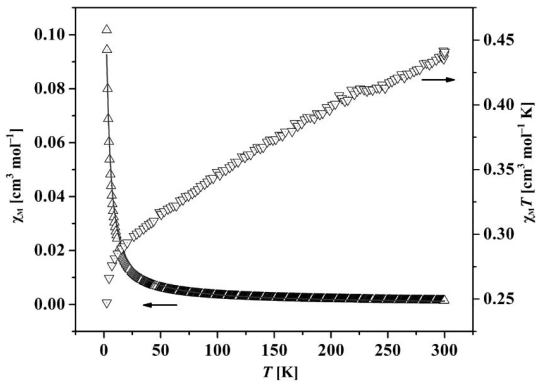

Figure 9. χ_M and $\chi_M T$ vs. T plot for **2**; the red line corresponds to the best fit obtained theoretically.

Conclusions

In this manuscript we presented the syntheses, novel crystallization procedure, structures, selective sorption properties, and variable-temperature magnetic properties (for **2**) of two metal–organic coordination frameworks of Cu^{II}. Framework solid **1** does not contain any regular channels and exhibits crystal-to-crystal transformation by the gaseous guest species MeOH under ambient conditions, which is rarely observed. Framework **2** contains supramolecular channels, and the desolvated framework of **2** also accommodates MeOH molecules effectively with structural transformations. Such kind of structural transformation and sorption was not observed with THF or C_6H_6 in either case, suggesting highly selective guest sorption. Desolvated frameworks **1′** and **2′** are both decorated with unsaturated metal sites, providing strong sorption affinity towards adsorbates having strong Lewis basic sites and a small size, such as MeOH, which can interact strongly with the pore surfaces, resulting in a substantial structural transformation, which is not effective for larger sized THF and C_6H_6 molecules. Weak antiferromagnetic coupling is observed in **2**, as expected from the *syn–anti* binding mode of the carboxylate groups.

Experimental Section

Materials: All the reagents and solvents employed were commercially available and used as supplied without further purification.

$Cu(NO_3)_2 \cdot 2H_2O$, 2,4-pyridinedicarboxylic acid, and 2,5-pyridinedicarboxylic acid were obtained from the Aldrich Chemical Co.

Physical Measurement: Elemental analyses were carried by using a Perkin–Elmer 2400 CHN analyzer. IR spectra of both compounds were recorded with a Bruker IFS 66v/S spectrophotometer by using KBr pellets in the region 4000–400 cm^{-1}. Thermogravimetric analysis (TGA) were carried out with a Mettler Toledo TGA850 instrument under a nitrogen atmosphere (flow rate of 50 $mL\,min^{-1}$) at a heating rate of 2 °C min^{-1}. X-ray powder diffraction (PXRD) pattern in different states of both samples were recorded with a Bruker D8 Discover instrument by using Cu-K_α radiation. Magnetic susceptibility measurements of compound **2** (300 –2.4 K) were performed with a vibrating sample magnetometer (VSM) in physical property measurement system (PPMS, Quantum Design, USA). N_2 and MeOH sorption isotherms were measured by using a Quantachrome Autosorb-1C analyzer at 77 and 298 K, respectively.

$[Na_2Cu(2,4\text{-pyrdc})(H_2O)(\mu\text{-}OH_2)_2]_n$ (1): An aqueous solution (15 mL) of $Cu(NO_3)_2 \cdot 2.5H_2O$ (0.232 g, 1 mmol) was added dropwise to an aqueous solution (5 mL) of the disodium salt of 2,4-pyridinedicarboxylic acid (0.229 g, 1 mmol). A sky-blue compound separated, and the resulting reaction mixture was stirred overnight under ambient conditions. The solution was filtered, and the blue filtrate was kept for slow evaporation; the sky-blue precipitate was discarded. Blue, square-block-type single crystals were obtained after 1 week, which were separated and washed with H_2O. Yield: 75%. IR (KBr): $\tilde{\nu}$ = 3424 (br.), 3151 (w), 3070 (w), 1658 (m), 1604 (m), 1556 (m), 1392 (s), 1091 (s), 890 (s) cm^{-1}. $C_{14}H_{12}CuN_2Na_2O_{11}$ (493.78): calcd. C 34.02, H 2.43, N 5.67; found C 34.67, H 2.87, N 5.15.

$\{[Cu(2,5\text{-pyrdc})(NH_3)](2H_2O)\}_n$ (2): An aqueous solution (10 mL) of $Cu(NO_3)_2 \cdot 2.5H_2O$ (0.232 g, 1 mmol) was added dropwise with constant stirring to an aqueous solution (25 mL) of a mixture of 2,5-pyridinedicarboxylic acid (0.164 g, 1 mmol) and KOH (0.056 g, 2 mmol). A sky-blue compound quantitatively precipitated, and the reaction mixture was stirred for 6 h. The resulting reaction mixture was filtered, and the sky-blue compound was treated with 14% aqueous NH_3 solution. The resulting clear, deep-blue solution was filtered and kept for slow evaporation. After 2 d blue crystals were separated and washed with H_2O. Yield: 65%. IR (KBr): $\tilde{\nu}$ = 3129 (w), 1670 (m), 1612 (m), 1390 (m), 1355 (m), 1041 (s) cm^{-1}. $C_7H_{10}CuN_2O_6$ (281.71): calcd. C 29.81, H 3.54, N 9.93; found C 30.31, H 3.33, N 9.78.

X-ray Crystallography: For each of **1** and **2**, a suitable blue-colored single crystal was mounted on a glass fiber and coated with epoxy resin. For **1**, X-ray single-crystal structural data was collected with a Bruker Smart-CCD diffractometer equipped with a normal focus, 2.4 kW sealed tube X-ray source (Mo-K_α radiation, λ = 0.71073 Å) operating at 50 kV and 30 mA. An empirical absorption correction based on symmetry-equivalent reflections was applied by using the SADABS program. For **2**, X-ray data collection was carried out with a Rigaku Mercury diffractometer with graphite monochromated Mo-K_α radiation (λ = 0.71069 Å) and a CCD 2D detector. In this case, the size of the unit cell was calculated from the reflections collected on the setting angles of seven frames by changing 0.5° for each frame. Three different settings were used and changed by 0.5° per frame, and the intensity data were collected with a scan width of 0.5°. Empirical absorption correction by using REQABA was performed for **2**. Both structures of **1** and **2** were solved by direct methods and followed by successive Fourier and difference Fourier syntheses. In both cases all the hydrogen atoms could be located in the difference Fourier map and included in the final refinement. All the non-hydrogen atoms in both cases were refined anisotropically. Final refinement included atomic positions for all the atoms, anisotropic thermal parameters for all the non-hydrogen atoms, isotropic thermal parameters for the hydrogen atoms. All calculations were carried out by using SHELXL 97,[25] SHELXS 97,[26] PLATON 99,[27] and WinGX system, Ver 1.70.01.[28] All crystallographic and structure refinements parameters for **1** and **2** are summarized in Table 3. Selected bond lengths, angles, and H-bonding parameters for **1** are given in the Supporting Information. Tables 1 and 2 displayed selected bond lengths, angles, and H-bonding parameters for **2**.

Table 3. Crystal and structure refinement data for **1** and **2**.

	$C_{14}H_{12}CuN_2Na_2O_{11}$	$C_7H_{10}CuN_2O_6$
M_r	493.79	281.72
Crystal system	monoclinic	triclinic
Space group	$P2_1/c$ (No. 14)	$P\bar{1}$ (No. 2)
a [Å]	16.0045(2)	4.9665(5)
b [Å]	8.3219(1)	7.807(5)
c [Å]	12.9712(2)	13.859(5)
α [°]	90	77.819 (5)
β [°]	103.2620(10)	75.709(5)
γ [°]	90	72.439(5)
V [Å^3]	1681.53(4)	491.0(6)
Z	4	2
T [K]	293	293
$D_{calcd.}$ [g cm^{-3}]	1.951	1.906
μ [mm^{-1}]	1.422	2.241
F (000)	996	286
θ_{max} [°]	26.5	30.1
λ (Mo-K_α) [Å]	0.71073	0.71073
Total data	14990	5402
Unique data, R_{int}	3474, 0.032	2317, 0.094
Data [$I > 2\sigma(I)$]	3097	2122
R[a],	0.0258	0.0528
R_w[b]	0.0713	0.1427
S	1.04	1.08

[a] $R = \Sigma||F_o| - |F_c||/\Sigma|F_o|$. [b] $R_w = [\Sigma\{w(F_o^2 - F_c^2)^2\}/\Sigma\{w(F_o^2)^2\}]^{1/2}$.

CCDC-711040 (for **2**) contains the supplementary crystallographic data for this paper. This data can be obtained free of charge from The Cambridge Crystallographic Data Centre via www.ccdc.ac.uk/data_request/cif.

Supporting Information (see footnote on the first page of this article): IR spectra of **1** and **2**; view of the rectangular-type channels with coordinatively unsaturated Cu^{II} sites in CPK model; TG analyses of **1** and **2**; N_2 sorption isotherm for **1** and **2**; color of **1** in different states; water sorption isotherm for **1′** and **2′**; PXRD pattern for **1** and **2** in different states; Selected bond lengths and bond angles for **1**; hydrogen bonds for **1**; powder indexing result of the dehydrated framework of **1** (**1′**) and **2** (**2′**).

Acknowledgments

T. K. M. is grateful to the Department of Science & Technology, Government of India, for financial assistance (Fast track scheme, SR/FTP/CS-46/2007). The Authors are thankful to Dr. G. Mostafa for valuable suggestions.

[1] a) S. R. Batten, R. Robson, *Angew. Chem. Int. Ed.* **1998**, *37*, 1460; b) P. J. Hagrman, D. Hagrman, J. Zubieta, *Angew. Chem. Int. Ed.* **1999**, *38*, 2638; c) B. Moulton, M. J. Zaworotko, *Chem. Rev.* **2001**, *101*, 1629; d) M. Eddaoudi, D. B. Moler, H. Li, B. Chen, T. M. Reineke, M. O'Keeffe, O. M. Yaghi, *Acc. Chem. Res.* **2001**, *34*, 319; e) C. Janiak, *Dalton Trans.* **2003**, 2781; f)

C. N. R. Rao, S. Natarajan, R. Vaidhyanathan, *Angew. Chem. Int. Ed.* **2004**, *43*, 1466.

[2] a) O. M. Yaghi, M. O'Keeffe, N. W. Ockwig, H. K. Chae, M. Eddaoudi, J. Kim, *Nature* **2003**, *423*, 705; b) S. Kitagawa, R. Kitaura, S.-I. Noro, *Angew. Chem. Int. Ed.* **2004**, *43*, 2334; c) S. E. James, *Chem. Soc. Rev.* **2003**, *32*, 276; d) D. Maspoch, D. Ruiz-Molina, J. Veciana, *J. Mater. Chem.* **2004**, *14*, 2713; e) G. Férey, C. Mellot-Draznieks, C. Serre, F. Millange, *Acc. Chem. Res.* **2005**, *38*, 217; f) G. Férey, *Chem. Soc. Rev.* **2008**, *37*, 191.

[3] a) J. L. C. Rowsell, O. M. Yaghi, *Angew. Chem. Int. Ed.* **2005**, *44*, 4670; b) X. Lin, J. Jia, X. Zhao, K. M. Thomas, A. J. Blake, G. S. Walker, N. R. Champness, P. Hubberstey, M. Schröder, *Angew. Chem. Int. Ed.* **2006**, *45*, 7358; c) M. Dincă, A. F. Yu, J. R. Long, *J. Am. Chem. Soc.* **2006**, *128*, 8904; d) S. Ma, D. Sun, J. M. Simmons, C. D. Collier, D. Yuan, H.-C. Zhou, *J. Am. Chem. Soc.* **2008**, *130*, 1012.

[4] a) S. Seo, D. Whang, H. Lee, S. L. Jun, J. Oh, Y. J. Jeon, K. Kim, *Nature* **2000**, *404*, 982; b) C.-D. Wu, A. Hu, L. Zhang, W. Lin, *J. Am. Chem. Soc.* **2005**, *127*, 8940.

[5] a) S. Kitagawa, M. Kondo, *Bull. Chem. Soc. Jpn.* **1998**, *71*, 1737; b) S. Kitagawa, K. Uemura, *Chem. Soc. Rev.* **2005**, *34*, 109; c) T. K. Maji, S. Kitagawa, *Pure Appl. Chem.* **2007**, *79*, 2155.

[6] a) M. P. Suh, J. W. Ko, H. J. Choi, *J. Am. Chem. Soc.* **2002**, *124*, 10976; b) K. Biradha, M. Fujita, *Angew. Chem. Int. Ed.* **2002**, *41*, 3392; c) S. Takamizawa, E.-i. Nakata, H. Yokoyama, K. Mochizuki, W. Mori, *Angew. Chem. Int. Ed.* **2003**, *42*, 4331; d) E. J. Cussen, J. B. Claridge, M. J. Rosseinsky, C. J. Kepert, *J. Am. Chem. Soc.* **2002**, *124*, 9574; e) G. H. Halder, C. J. Kepert, B. Moubaraki, K. S. Murray, J. D. Cashion, *Science* **2002**, *298*, 1762.

[7] a) K. Uemura, S. Kitagawa, M. Kondo, K. Fukui, R. Kitaura, H.-C. Chang, T. Mizutani, *Chem. Eur. J.* **2002**, *8*, 3586.

[8] a) K. Biradha, Y. Hongo, M. Fujita, *Angew. Chem. Int. Ed.* **2002**, *41*, 3395; b) H. J. Choi, M. P. Suh, *J. Am. Chem. Soc.* **2004**, *126*, 15844; c) R. Matsuda, R. Kitaura, S. Kitagawa, Y. Kubota, T. C. Kobayashi, S. Horike, M. Takata, *J. Am. Chem. Soc.* **2004**, *126*, 14063; d) C. Serre, F. Millange, C. Thouvenot, M. Nogues, G. Marsolier, D. Louer, G. Férey, *J. Am. Chem. Soc.* **2002**, *124*, 13519.

[9] a) D. Bradshaw, T. J. Prior, E. J. Cussen, J. B. Claridge, M. J. Rosseinsky, *J. Am. Chem. Soc.* **2004**, *126*, 6106; b) L. Pan, K. M. Adams, H. E. Hernandez, X. Wang, C. Zheng, Y. Hattori, K. Kaneko, *J. Am. Chem. Soc.* **2003**, *125*, 3062; c) T. K. Maji, R. Matsuda, S. Kitagawa, *Nat. Mater.* **2007**, *6*, 142; d) D. N. Dybtsev, H. Chun, S. H. Yoon, D. Kim, K. Kim, *J. Am. Chem. Soc.* **2004**, *126*, 32.

[10] a) B. Chen, M. Eddaoudi, T. M. Reineke, T. W. Kampf, M. O'Keeffe, O. M. Yaghi, *J. Am. Chem. Soc.* **2000**, *122*, 11559; b) B. Chen, N. W. Ockwig, A. R. Millward, D. S. Contreras, O. M. Yaghi, *Angew. Chem. Int. Ed.* **2005**, *44*, 4745; c) K. Takaoka, M. Kawano, M. Tominaga, M. Fujita, *Angew. Chem. Int. Ed.* **2005**, *44*, 2151; d) P. D. C. Dietzel, R. E. Johnsen, H. Fjellvag, S. Bordiga, E. Groppo, S. Chavan, R. Blom, *Chem. Commun.* **2008**, 5125; e) A. C. McKinlay, B. Xiao, D. S. Wragg, P. S. Wheatley, I. L. Megson, R. E. Morris, *J. Am. Chem. Soc.* **2008**, *130*, 10440; f) B. Panella, M. Hirscher, H. Pütter, U. Müller, *Adv. Funct. Mater.* **2006**, *16*, 520; g) P. M. Forster, J. Eckert, B. D. Heiken, J. B. Parise, J. W. Yoon, S. H. Jhung, J.-S. Chang, A. K. Cheetham, *J. Am. Chem. Soc.* **2006**, *128*, 16846; h) M. Dincă, J. R. Long, *J. Am. Chem. Soc.* **2005**, *127*, 9376; i) M. Dinca, A. Dailly, Y. Liu, C. M. Brown, D. A. Neumann, J. R. Long, *J. Am. Chem. Soc.* **2006**, *128*, 16876; j) K. Schlichte, T. Kratzke, S. Kaskel, *Microporous Mesoporous Mater.* **2004**, *73*, 81; k) O. Ohmori, M. Fujita, *Chem. Commun.* **2004**, 1586; l) H. R. Moon, N. Kobayashi, M. P. Suh, *Inorg. Chem.* **2006**, *45*, 8672; m) Y. Liu, H. Kabbour, C. M. Brown, D. A. Neumann, C. C. Ahn, *Langmuir* **2008**, *24*, 4772.

[11] a) R. Kitaura, K. Seki, G. Akiyama, S. Kitagawa, *Angew. Chem. Int. Ed.* **2003**, *42*, 428; b) K. Seki, *Phys. Chem. Chem. Phys.* **2002**, *4*, 1968; c) D. Li, K. Kaneko, *Chem. Phys. Lett.* **2001**, *335*, 50; d) S. Takamizawa, E.-i. Nakata, H. Yokoyama, K. Mochizuki, W. Mori, *Angew. Chem. Int. Ed.* **2003**, *42*, 4331; e) R. Kitaura, K. Fujimoto, S.-i. Noro, M. Kondo, S. Kitagawa, *Angew. Chem. Int. Ed.* **2002**, *41*, 133; f) K. Uemura, S. Kitagawa, K. Fukui, K. Saito, *J. Am. Chem. Soc.* **2004**, *126*, 3817; g) A. Kondo, H. Niguchi, L. Carlucci, D. M. Proserpio, G. Ciani, H. Kajiro, T. Ohba, H. Kanoh, K. Kaneko, *J. Am. Chem. Soc.* **2007**, *129*, 12362; h) S. Bourrelly, P. L. Llewellyn, C. Serre, F. Milange, T. Loiseau, G. Férey, *J. Am. Chem. Soc.* **2005**, *127*, 13519.

[12] a) T. K. Maji, G. Mostafa, R. Matsuda, S. Kitagawa, *J. Am. Chem. Soc.* **2005**, *127*, 17152; b) M. Albrecht, M. Lutz, A. L. Spek, G. van Koten, *Nature* **2000**, *406*, 970; c) S. Supriya, S. K. Das, *J. Am. Chem. Soc.* **2007**, *129*, 3464; d) A. Lennartson, M. Hakkanson, S. Langer, *New. J. Chem.* **2007**, *31*, 344; e) G. M. Espallargas, M. Hippler, A. J. Florence, P. Fernandes, J. v. d. Streek, M. Brunelli, W. I. F. David, K. Shankland, L. Brammer, *J. Am. Chem. Soc.* **2007**, *129*, 15606.

[13] a) L. G. Beauvais, M. P. Shores, J. R. Long, *J. Am. Chem. Soc.* **2000**, *122*, 2763; b) D. Bradshaw, J. E. Warren, M. J. Rosseinsky, *Science* **2007**, *315*, 977.

[14] E. E. Sileo, G. Rigotti, O. E. Piro, *Acta Chem. Scand.* **1999**, *53*, 535.

[15] K. Nakamoto, *Infrared and Raman Spectra of Inorganic and Coordination compounds*, 5th ed., John Wiley & Sons, **1997**.

[16] S.-I. Noro, H. Miyasaka, S. Kitagawa, T. Wada, T. Okubo, M. Yamashita, T. Mitani, *Inorg. Chem.* **2005**, *44*, 133.

[17] The size was measured by considering the van der Waals radii for the constituting atoms. Hereafter, all size estimations of the pores is performed in this way.

[18] P.-E. Werner, L. Eriksson, M. Westdahl, *J. Appl. Crystallogr.* **1985**, *18*, 367.

[19] The molecular area was calculated from liquid density by assuming spherical symmetry and hexagonal close packing. The equation and values are given in ref.[20]

[20] C. E. Webster, R. S. Drago, M. C. Zerner, *J. Am. Chem. Soc.* **1998**, *120*, 5509.

[21] M. M. Dubinin, *Chem. Rev.* **1960**, *60*, 235.

[22] D. Min, S. S. Yoon, D.-Y. Jung, C. Y. Lee, Y. Kim, W. S. Han, S. W. Lee, *Inorg. Chim. Acta* **2001**, *324*, 293.

[23] a) J. C. Bonner, M. E. Fischer, *Phys. Rev. A* **1964**, *135*, 640; b) W. E. Estes, D. P. Havel, W. E. Hatfield, D. Hodgson, *Inorg. Chem.* **1978**, *17*, 1415.

[24] a) C. Ruiz-Pérez, J. Sanchiz, M. Hernández-Molina, F. Lloret, M. Julve, *Inorg. Chem.* **2000**, *39*, 1363; b) S. Sain, T. K. Maji, G. Mostafa, T. H. Lu, N. R. Chaudhuri, *New J. Chem.* **2003**, *27*, 185; c) J. Pasán, J. Sanchiz, C. Ruiz-Pérez, F. Lloret, M. Julve, *Inorg. Chem.* **2005**, *44*, 7794; d) A. Rodriguez-Fortea, P. Alemany, S. Álvarez, E. Ruiz, *Chem. Eur. J.* **2001**, *7*, 627; e) J. Pasán, J. Sanchiz, F. Lloret, M. Julve, C. Ruiz-Pérez, *CrystEngComm* **2007**, *9*, 478; f) R. Baldomá, M. Monfort, J. Ribas, X. Solans, M. A. Maestro, *Inorg. Chem.* **2006**, *45*, 8144.

[25] G. M. Sheldrick, *SHELXL 97: Program for the Solution of Crystal Structure*, University of Gottingen, Germany, **1997**.

[26] G. M. Sheldrick, *SHELXS 97: Program for the Solution of Crystal Structure*, University of Gottingen, Germany, **1997**.

[27] A. L. Spek, *PLATON: Molecular Geometry Program*, University of Utrecht, The Netherlands, **1999**.

[28] WinGX – A Windows Program for Crystal Structure Analysis: L. J. Farrugia, *J. Appl. Crystallogr.* **1999**, *32*, 837.

Received: November 27, 2008
Published Online: March 22, 2009

